

# Modeling anisotropic sensitivity in pentaerythritol tetranitrate using strain rate dependent detonation rate law

Kihong Kim<sup>1,2</sup>, Laurence E. Fried<sup>2</sup> and Jack J. Yoh<sup>1</sup>

<sup>1</sup> School of Mechanical and Aerospace Engineering, Seoul National University  
Seoul 151-744, Korea

<sup>2</sup> Lawrence Livermore National Laboratory  
Livermore, CA 94551, USA

## 1 Introduction

An anisotropic sensitivity of detonation under mechanical impact of high explosive has shown preferred direction of crystal orientation on shock initiation experiment of single crystals of pentaerythritol tetranitrate (PETN) [1-3]. For instance, the pressure threshold for detonation for PETN crystals along the  $\langle 100 \rangle$  direction is at least 4 times that for  $\langle 110 \rangle$  direction [4]. Recently, Plaksin [5] provided experimental evidence that the maximum shear stress leads to preferential sensitivity to detonation.

Experimental findings [1-3,5] and molecular simulations [4,6,7] both suggest that special coupling between thermal, chemical, and mechanical effects is necessary to properly address realistic mechanism of anisotropic sensitivity in a single crystal PETN. In a larger scale, a continuum model based on the phase-field theory was suggested [8] to embrace the physical elements and sub models that may describe an anisotropic energetic crystal undergoing phase transition.

Table 1 summarizes various input stresses for different crystal orientations for go/no-go transition to detonation. Both  $\langle 110 \rangle$  and  $\langle 001 \rangle$  directions are shown to be sensitive to impact even at relatively low pressure of 8.6 GPa while  $\langle 101 \rangle$  and  $\langle 100 \rangle$  directions exhibit insensitivity to stresses even up to 19.5 GPa. This anomalous characteristics observed in experiment has been explained by the steric hindrance effect [2] in the microscopic concept. The steric hindrance model consists of dislocation and preferred slip planes induced by the micro structure of PETN.

In the continuum model of detonation rate laws, the ignition and growth (I & G) model [9] based on empirical observation on the pressure-dependent initiation of detonation has been widely used to date. The basis of the model is the hot spot theory where inclusion of compressibility (or density) factor to ignite heterogeneous high explosives is noted. Since the model is essentially independent of direction of compression, that is, isotropic; it is impossible to address sensitivity associated with preferred orientation for building a go/no-go condition. In this paper, we provide a model that incorporates what has been observed in experiments and atomistic calculations of PETN and proposed a crystal

orientation dependent reactive flow model. A general tensor notation is utilized to fully address three-dimensional effect of strain rate dependence to the chemical response of high explosive. This allows for a meaningful coupling of thermal and mechanical behavior of HE in the global balance laws of any energetic materials.

Table 1: PETN shock initiation data [1]

Shock direction	Input stress (GPa)	Run distance to detonation (mm)
<110>	8.6	7.3
	12.4	4.6
<001>	12.4	9.5
<101>	8.6	No go below 19.5 GPa
<100>	12.4	No go below 19.5 GPa

## 2 Anisotropic chemical kinetics

A direction-dependent detonation rate law in a tensor form is defined by

$$\frac{\partial \lambda}{\partial t} + \frac{\partial \lambda u_i}{\partial x_i} = I(1-\lambda)^b \left[ (\varepsilon_{ij} \beta_{ij} - A_{ij} \delta_{ij}) H(\dot{\varepsilon}_{ij}) \right]^x + G(1-\lambda)^c \lambda^d p^y \quad (1)$$

where the reaction progress variable  $\lambda$ , the strain tensor  $\varepsilon_{ij}$ , the strain rate tensor  $\dot{\varepsilon}_{ij}$ , anisotropic coefficient tensor  $\beta_{ij}$ , constant matrix tensor  $A_{ij}$ , and a Heaviside step function  $H(\dot{\varepsilon}_{ij})$  are given as follows

$$A_{ij} \equiv \begin{pmatrix} 1 & \frac{1}{2} & \frac{1}{2} \\ \frac{1}{2} & 1 & \frac{1}{2} \\ \frac{1}{2} & \frac{1}{2} & 1 \end{pmatrix}, \quad \beta_{ij} = \begin{pmatrix} \frac{A_{11}}{\varepsilon_{xx,0}} & \frac{A_{12}}{\varepsilon_{xy,0}} & \frac{A_{13}}{\varepsilon_{xz,0}} \\ \frac{A_{21}}{\varepsilon_{yx,0}} & \frac{A_{22}}{\varepsilon_{yy,0}} & \frac{A_{23}}{\varepsilon_{yz,0}} \\ \frac{A_{31}}{\varepsilon_{zx,0}} & \frac{A_{32}}{\varepsilon_{zy,0}} & \frac{A_{33}}{\varepsilon_{zz,0}} \end{pmatrix},$$

$$\varepsilon_{ij} = \begin{pmatrix} \varepsilon_{xx} & \varepsilon_{xy} & \varepsilon_{xz} \\ \varepsilon_{yx} & \varepsilon_{yy} & \varepsilon_{yz} \\ \varepsilon_{zx} & \varepsilon_{zy} & \varepsilon_{zz} \end{pmatrix}, \quad \dot{\varepsilon}_{ij} = \frac{1}{2} \left( \frac{\partial u_i}{\partial x_j} + \frac{\partial u_j}{\partial x_i} \right), \quad H(\dot{\varepsilon}_{ij}) = \begin{cases} 1 & \text{if once } \dot{\varepsilon}_{ij} \geq \dot{\varepsilon}_{ij,0} \\ 0 & \text{otherwise} \end{cases}. \quad (2)$$

The first term in the RHS of Eq. (1) is ignition term controlled by the anisotropic coefficient tensor and strain rate corresponding to mechanical input, while the second term describes the growth phase of reaction governed by the pressure. The values of the reference strain rate,  $\dot{\varepsilon}_{ij,0}$ , are defined in an intrinsic sense of physical regime, such that their typical values are given in Table 2. The typical range of the detonation regime is between  $10^7 \sim 10^8$  /s.

Table 2: Regime of physical strain rates [10]

Strain rate (1/s)	Impact velocity (m/s)	Effect
$< 10^{-5}$		Creep
$10^{-5} - 10^{-1}$		Elastic

$10^{-1} - 10^1$	$< 50$	Primarily elastic
$10^1 - 10^3$	$50 - 500$	Primarily plastic
$10^3 - 10^5$	$500 - 1000$	Local plasticity, material strength significant
$10^5 - 10^6$	$1000 - 3000$	Pressure exceeds or approaches material strength
$10^6 - 10^8$	$3000 - 12000$	Pressure is many times the material strength
$> 10^8$	$> 12000$	Vaporization of colliding solids

In the Eulerian framework, the rate law can be explicitly written out as follows

$$\begin{aligned} & \frac{\partial \lambda}{\partial t} + \frac{\partial \lambda u}{\partial x} + \frac{\partial \lambda v}{\partial y} + \frac{\partial \lambda w}{\partial z} = \\ I(1-\lambda)^b & \left[ \left( \frac{\varepsilon_{xx}}{\varepsilon_{xx,0}} - 1 \right) H(\dot{\varepsilon}_{xx}) + \left( \frac{\varepsilon_{yy}}{\varepsilon_{yy,0}} - 1 \right) H(\dot{\varepsilon}_{yy}) + \left( \frac{\varepsilon_{zz}}{\varepsilon_{zz,0}} - 1 \right) H(\dot{\varepsilon}_{zz}) + \left( \frac{\varepsilon_{xy}}{\varepsilon_{xy,0}} - 1 \right) H(\dot{\varepsilon}_{xy}) \right. \\ & \left. + \left( \frac{\varepsilon_{yz}}{\varepsilon_{yz,0}} - 1 \right) H(\dot{\varepsilon}_{yz}) + \left( \frac{\varepsilon_{zx}}{\varepsilon_{zx,0}} - 1 \right) H(\dot{\varepsilon}_{zx}) \right]^x + G_1(1-\lambda)^c \lambda^d p^y + G_2(1-\lambda)^e \lambda^g p^z. \quad (3) \end{aligned}$$

Ignition is sensitive to resulting coupling between input strength and the ratio of strain to reference strain as

$$\frac{\varepsilon_{ij}}{\varepsilon_{ij,0}} = \begin{cases} \frac{\varepsilon_{ij}}{\varepsilon_{ij,0}} & \text{if } \varepsilon_{ij} \geq \varepsilon_{ij,0} \\ 1 & \text{otherwise} \end{cases}. \quad (4)$$

The physically strain rate represents the type of mechanical input, for instance static, ramp, or step compression, subjected to a PETN in Fig. 1. A shock impact is described by a step function, commonly associated with an impact applied to PETN test. The strain rate function  $H(\dot{\varepsilon}_{ij})$  with respect to a coordinate direction permits go/no go condition for ignition. The threshold strain rate is low in sensitive orientation while it is high in insensitive orientation. The strain ratio is physically equivalent to a density ratio in the point of compressibility that explains ignition induced by hot spots [9].

The idealized or isotropic behavior captured via the classical I & G framework can be naturally recovered if one applies constant values for all reference strain and strain rates of the anisotropic coefficient tensor as follows,

$$\beta_{ij} = \frac{1}{\varepsilon_0} A_{ij} = \frac{1}{\varepsilon_0} \begin{pmatrix} 1 & \frac{1}{2} & \frac{1}{2} \\ \frac{1}{2} & 1 & \frac{1}{2} \\ \frac{1}{2} & \frac{1}{2} & 1 \end{pmatrix} \text{ and } \dot{\varepsilon}_{ij,0} = \dot{\varepsilon}_0 \begin{pmatrix} 1 & 1 & 1 \\ 1 & 1 & 1 \\ 1 & 1 & 1 \end{pmatrix}. \quad (5)$$

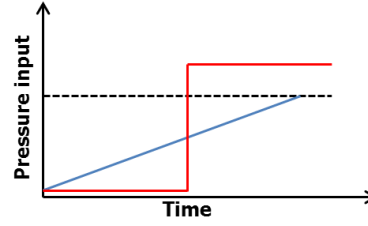


Figure 1. A variety of pressure loading or strain rate based compression on the initial impact of high explosive (Static, Ramp, Step)

### 3 Governing equations

The governing equations involving mass, momentum, energy conservation and species evolution in two-dimensional cylindrical coordinate are defined by

$$\frac{\partial \rho}{\partial t} + \frac{\partial \rho u_r}{\partial r} + \frac{\partial \rho u_z}{\partial z} = 0, \quad (6)$$

$$\frac{\partial \rho u_r}{\partial t} + \frac{\partial (\rho u_r^2 + p)}{\partial r} + \frac{\partial \rho u_r u_z}{\partial z} = 0, \quad (7)$$

$$\frac{\partial \rho u_z}{\partial t} + \frac{\partial \rho u_r u_z}{\partial r} + \frac{\partial (\rho u_z^2 + p)}{\partial z} = 0, \quad (8)$$

$$\frac{\partial \rho E}{\partial t} + \frac{\partial u_r (\rho E + p)}{\partial r} + \frac{\partial u_z (\rho E + p)}{\partial z} = 0, \quad (9)$$

$$\begin{aligned} \frac{\partial \lambda}{\partial t} + \frac{\partial \lambda u_r}{\partial r} + \frac{\partial \lambda u_z}{\partial z} = & I(1-\lambda)^b \left[ \left( \frac{\varepsilon_{rr}}{\varepsilon_{rr,0}} - 1 \right) \chi_{rr} (\dot{\varepsilon}_{rr}) + \left( \frac{\varepsilon_{zz}}{\varepsilon_{zz,0}} - 1 \right) \chi_{zz} (\dot{\varepsilon}_{zz}) + \left( \frac{\varepsilon_{rz}}{\varepsilon_{rz,0}} - 1 \right) \chi_{rz} (\dot{\varepsilon}_{rz}) \right]^x \\ & + G_1 (1-\lambda)^c \lambda^d p^y + G_2 (1-\lambda)^e \lambda^g p^z \\ & 0 < F < F_{\text{igmax}}, \quad 0 < F < F_{\text{G1max}}, \quad F_{\text{G2min}} < F < 1. \end{aligned} \quad (10)$$

where  $\rho$  is density,  $u_r$ ,  $u_z$  are velocity components in radial and axial directions,  $E$  is the total energy per unit mass with  $e$  being its specific internal energy, and  $p$  is the hydrostatic pressure. We assume that (i) dislocation and slip system in molecular scale are neglected; instead strain and strain rate dependent ignition is enforced, (ii) orientation-dependent initiation of detonation is governed by the impact (pressure) direction, (iii) elastic-plastic behavior is negligible for strong shock wave assumption in the early stages of simulation such that the stress fields are unchanged during that time, (iv) explosive runaway or growth phase is mostly pressure driven.

The JWL equation of state (EOS) is used to model explosives in the high pressure regime as follow

$$p = A(1 - \omega R_1 / V) e^{-R_1 v} + B(1 - \omega R_2 / V) e^{-R_2 v} + \frac{\omega E}{V}. \quad (11)$$

Table 3 and 4 summarize the chemical kinetics parameters and the EOS of PETN for the numerical simulation. For more in-depth description of the numerical implementation of the model, readers are referred to [11].

Table 3: Parameters for anisotropic rate law

$I$ (1/ $\mu\text{s}$ )	100
$b, c, e, g$	0.667

$d$	0.01
$\varepsilon_{rr}, \varepsilon_{zz}, \varepsilon_{rz}$	-0.199
$x$	8
$G_1$ (Mbar <sup>-y</sup> / $\mu\text{s}$ )	0.15

$y$	1	$B$ [GPa]	-3.752	90.570
$G_2$ (Mbar <sup>-y</sup> /μs)	1500	$R_1$	10	6
$z$	2	$R_2$	1	2.6
$F_{igmax}$	0.01	$\omega$	0.568	0.57
$F_{G1max}$	0.01	$C_v$ [GPa/K]	2.718e-3	1e-3
$F_{G2min}$	0.01	$T_0$ [K]	298	-
$\dot{\epsilon}_{rr,0}$ (1/μs)	-1600	$E_0$ [GPa]	0	10.8
$\dot{\epsilon}_{zz,0}$ (1/μs)	-4200			
$\dot{\epsilon}_{rz,0}$ (1/μs)	-4200			

Table 4: Equation of state for PETN

	Unreacted	Reacted
$A$ [GPa]	20208	1032.258

## 4 Results

The one dimensional numerical simulations for PETN based on both original I & G and the present anisotropic rate law are carried out to validate the proposed mechanism of directional sensitivity in the PETN. Two different rate laws (traditional vs. anisotropic) are written for a quick comparison:

$$\frac{\partial \lambda}{\partial t} + \frac{\partial \lambda u}{\partial x} = I(1-\lambda)^b \left( \frac{\rho}{\rho_0} - 1 - a \right)^x + G_1(1-\lambda)^c \lambda^d p^y + G_2(1-\lambda)^e \lambda^g p^z, \quad (12)$$

$$\frac{\partial \lambda}{\partial t} + \frac{\partial \lambda u}{\partial x} = I(1-\lambda)^b \left[ \left( \frac{\epsilon_{rr}}{\epsilon_{rr,0}} - 1 \right) \chi_{rr}(\dot{\epsilon}_{rr}) \right]^x + G_1(1-\lambda)^c \lambda^d p^y + G_2(1-\lambda)^e \lambda^g p^z. \quad (13)$$

The classical I & G parameters for PETN are from [9]. A uniform mesh of 2.5 μm/mesh is used and a wide range of impact pressure of 8 to 19 GPa are subjected to one end of PETN in its sensitive direction. The calculated distance to detonation showing shock wave overtaken by the reaction front is compared with experimental and other numerical data [3,9,12] in Fig. 2. The present anisotropic rate law reproduces exactly experimental records in entire domain, however there shows a discrepancy in the region of relatively high pressure input. One peculiar aspect of PETN detonation is existence of a super detonation [1] where the pre-compressed PETN accelerates the reaction rate. Pressure and shock velocity in the super detonation regime are higher than the C-J values, as illustrated in Fig. 3. For impact pressure 8 GPa, the time evolution graphs for both pressure and reaction progress in Figs. 4 and 5 clearly mark the von Neumann spike at 45 GPa. The Chapman-Jouguet (CJ) pressure of 33 GPa is also in good agreement with experimental data. Therefore, the 1-D anisotropic model is shown to capture the features of both ideal I & G result and the experimental data.

The confined rate stick test [11] consisting of a copper tube filled with an explosive charge is performed in the two-dimensional anisotropic detonation simulation. Computational domain is 0.06 m × 0.1 m and a uniform mesh distribution of eight meshes/mm is used in the simulation. An impact speed of 3,000 m/s is head on to a one end of explosive along the  $zz$  direction. Two representative sensitive directions in a cylindrical coordinate considered are; (i) sensitive in the  $zz$  direction  $\langle 001 \rangle$ , and (ii) sensitive in the  $rz$  direction  $\langle 011 \rangle$ . Figure 6 shows noticeable differences in the pressure and progress variable depending on the direction of shock impact. The chemical reaction is triggered by relatively small reference strain rates when the shock travels along the sensitive direction, namely  $\langle 001 \rangle$ . When a shock moves perpendicular and skew to the charge, a detonation failure is observed. In case (ii), detonation runaway is not observed since the strain rate  $\dot{\epsilon}_{zz}$ , in the direction of shock wave is

always less than the reference strain rate,  $\dot{\epsilon}_{zz,0}$ . Figure 7 also shows a full detonation development in (i) while a failure is observed in (ii). Results show that the proposed rate model is suitable for manipulating the anisotropic sensitivity in any target explosive material under investigation, not limited to PETN.

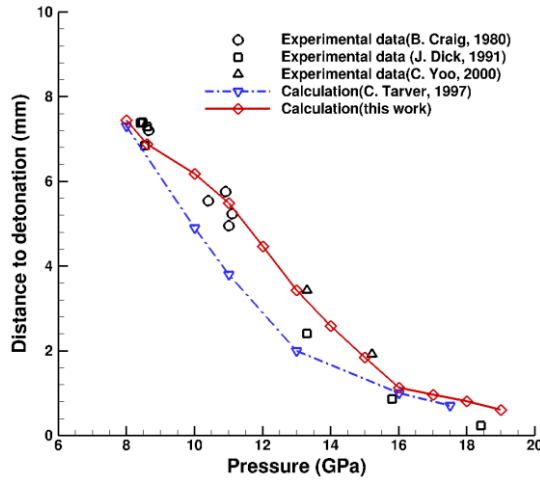


Figure 2. Distance to detonation vs. input shock stress of PETN in the sensitive orientation

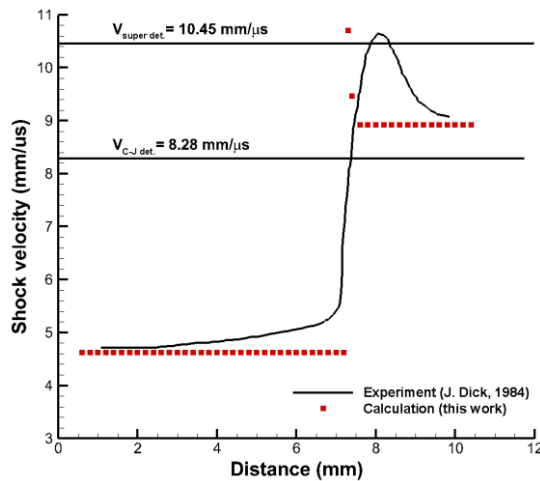


Figure 3. Shock velocity vs. run distance for PETN crystals shocked at 8.6 GPa

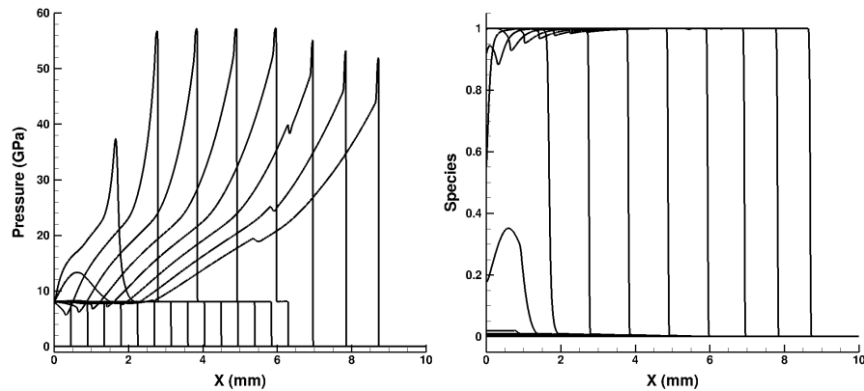


Figure 4. 1D test of ignition and growth model for PETN (ideal case)

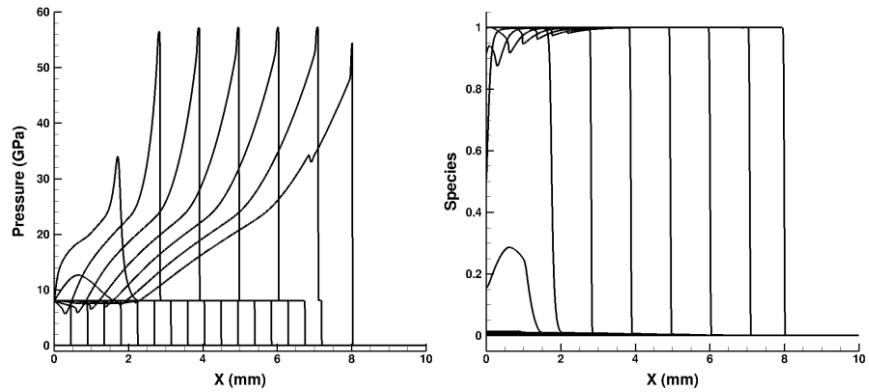


Figure 5. 1D test of anisotropic model for PETN.

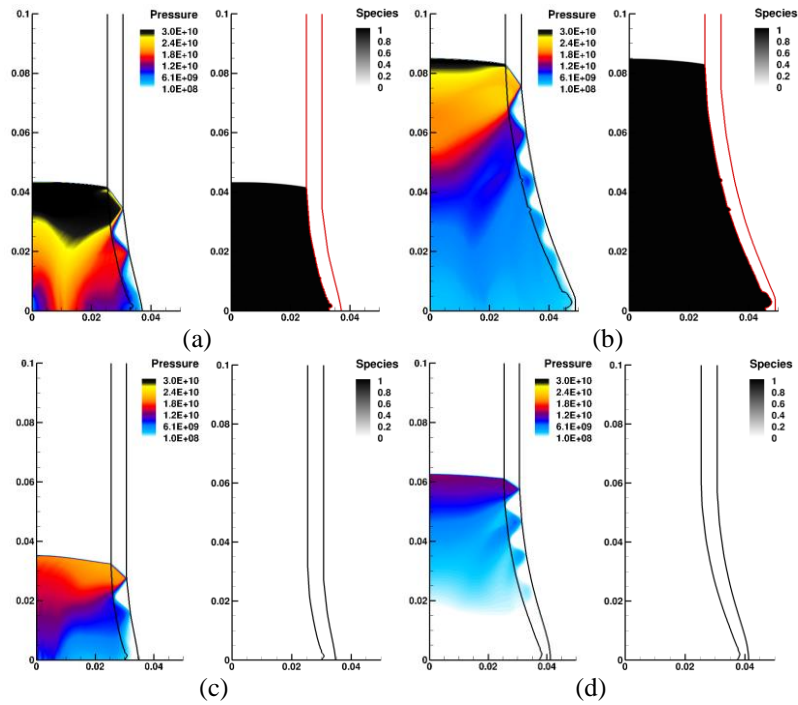
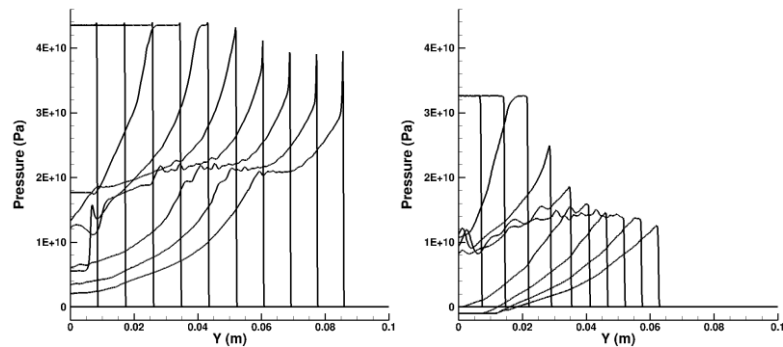


Figure 6. 2D anisotropic sensitivity test for PETN confined in a copper tube at 5 and 10  $\mu$ s: (a, b) Pressure and progress variable in  $\langle 001 \rangle$ , (c, d) Pressure and progress variable in  $\langle 011 \rangle$ .



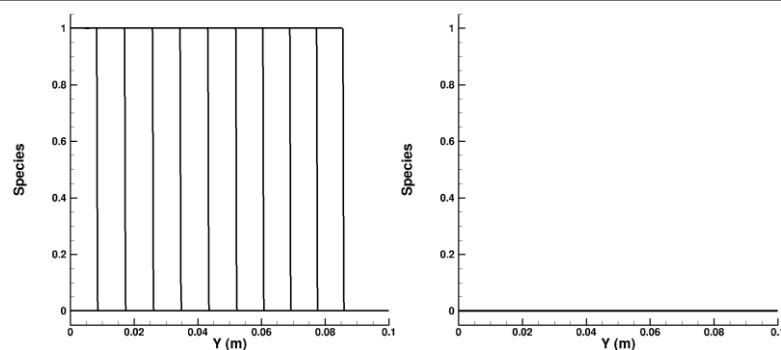


Figure 7. Pressure and reaction progress evolution shown along a sensitive direction  $\langle 001 \rangle$  direction sensitive case showing full detonation (LEFT), and  $\langle 011 \rangle$  direction showing detonation failure (RIGHT): (upper) pressure, (bottom) species.

## 5 Conclusion

We have presented and validated a new anisotropic detonation rate model for general ignition behavior of PETN. Inclusion of strain tensor allows for direction sensitivity to ignition of PETN. 1D tests reproduced the experimental data as well as idealized (isotropic) I & G results. 2D rate stick test validated the anisotropic detonation of PETN upon direction sensitive impacts. The proposed model is expected to enhance the fidelity of the current state of direction sensitive detonation modeling.

## References

- [1] Dick J.J. (1984). Effect of crystal orientation on shock initiation sensitivity of pentaerythritol tetranitrate explosive. *Appl. Phys. Lett.* 44: 859.
- [2] Dick J.J. (1997). Anomalous shock initiation of detonation in pentaerythritol tetranitrate crystals. *J. Appl. Phys.* 81: 601.
- [3] Yoo C.S., Holmes N.C., Souers P.C., Wu C.J., Ree F.H., Dick J.J. (2000). Anisotropic shock sensitivity and detonation temperature of pentaerythritol tetranitrate single crystal. *J. Appl. Phys.* 88: 70.
- [4] Zybin S.V., Goddard III W.A., Xu P., van Duin A.C.T., Thompson A.P. (2010). Physical mechanism of anisotropic sensitivity in pentaerythritol tetranitrate from compressive-shear reaction dynamics simulations. *Appl. Phys. Lett.* 96: 081918.
- [5] Plaskin I., Coffey C.S., Mendes R., Ribeiro J., Campos J., Direito J. 13<sup>th</sup> Symp. on Detonation, ONR 351-07-01, 2006, p. 319
- [6] Gruzdkov Y.A., Gupta Y.M. (2000). Shock wave initiation of pentaerythritol tetranitrate single crystals: mechanism of anisotropic sensitivity. *J. Phys. Chem.* 104: 11169.
- [7] Maffre P., Peyrard M. (1992). Molecular-dynamics investigations of shock-induced detonations in inhomogeneous energetic crystals. *Phys. Rev. B* 45: 9551.
- [8] Stewart D.S., Fried L.E., Szuck M. (2011) Shock Compression of Condensed Matter AIP Conf. Proc. 1426, 263-266; doi: 10.1063/1.3686269
- [9] Lee E.L., Tarver C.M. (1980). Phenomenological model of shock initiation in heterogeneous explosives. *Phys. Fluids.* 23: 2362.
- [10] U. S. Lindholm, High strain rate tests. *Techniques of Metals Research* 5, Part 1. Wiley, New York, (1971).
- [11] Kim K., Yoh J.J. (2013). A particle level-set based Eulerian method for multi-material detonation simulation of high explosive and metal confinements. *P. Combust. Inst.* 34: 2025.
- [12] Dick J., Mulford R., Spencer W, Pettit D., Garcia E., and Shaw D. (1991). Shock response of pentaerythritol tetranitrate single crystals. *J. Appl. Phys.* 70: 3572.